[16] D. D. Tang and R. J. Lomax, "Bias-tuning and modulation characteristics of transferred-electron oscillators," *IEEE Trans. Microwave Theory Tech.*, vol. MTT-23, pp. 748–753, Oct. 1975.
[17] W. C. Tsai and F. J. Rosenbaum, "Amplitude and frequency modulation of a waveguide cavity CW Gunn oscillator," *IEEE Trans. Microwave Theory Tech.*, vol. MTT-18, pp. 877–884, Nov. 1970.
[18] G. King and M. P. Wasse, "Frequency modulation of Gunn effect oscillators," *IEEE Trans. Electron Devices*, vol. ED-14 (Corr.), pp. 717–718, Oct. 1967.

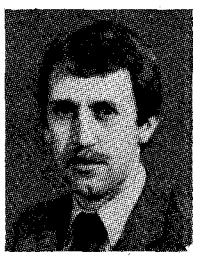

Peter A. Jefford was born in Manchester, England on August 18, 1955. He received the B.Sc. degree in electrical and electronic engineering from the University of Leeds in 1976 and completed a Ph.D. degree on modulation schemes in microwave field sensors at the same University in 1980.

Since 1980 he has been working at the Royal Signals and Radar Establishment, Malvern, England, engaged in microwave and millimeter-wave subsystems research.

Dr. Jefford is an associate member of the Institute of Electrical Engineers, London.

Michael J. Howes was born in Lowestoft, England, in 1941, and acquired his early education while working at a Government Fisheries Research Station where he was involved in the development of sector scanning sonar systems. He received the B.Sc. and Ph.D. degrees from the University of Leeds, England, in 1965 and 1967 respectively.

He is presently a Senior Lecturer in the Department of Electrical and Electronic Engineering at the University of Leeds, and has acted as consultant to a number of companies in the U.K. and U.S.A.

During the period 1981–1982 he was the Technical Director of MM Microwave, Ltd. His research interests are in the areas of microwave solid-state devices and systems in general, and his personal research work is currently associated with the design of MESFET amplifiers, oscillators, and mixers.

Dr. Howes is a Fellow of the Institute of Electrical Engineers and a member of the Institute of Physics.

Measurement and Modeling of the Apparent Characteristic Impedance of Microstrip

WILLIAM J. GETSINGER, FELLOW, IEEE

Abstract—**Voltage and current cannot be defined uniquely for microstrip except at zero frequency, and therefore microstrip has not been rigorously incorporated into circuit theory. However, in engineering practice, microstrip exhibits an apparent characteristic impedance, denoted here by *ZA*, that can be measured.**

Three methods of measuring *ZA* were devised and used in measuring three impedance levels of microstrip. These methods are described and experimental results presented. The measurements of *ZA* were found to be consistent with the power-current characteristic impedance definition of the approximate longitudinal-section electric (LSE) model of microstrip. Simple approximate formulas for representing *ZA* are also discussed.

I. Introduction

IMPEDANCE IS a fundamental concept in microwave circuit design because the impedances of circuit elements and their interconnections determine the distribution of power within a circuit. The ability of a microwave engineer to predict circuit performance will partially depend on the accuracy of the knowledge of impedances for available circuit elements.

This paper examines the frequency variation of the apparent characteristic impedance of a microstrip transmission line. From a practical viewpoint, the term "characteristic impedance" used here is the impedance parameter of a circuit-theory based model of a transmission line which is used in a circuit description with other elements to predict the actual performance of a physical circuit. An example is the parameter *Z*0 used in a computer-aided design (CAD) program, such as SUPER-COMPACT™. Microstrip is not a TEM line, and so voltage and current, and thus characteristic impedance, cannot be defined uniquely. The term "apparent characteristic impedance" is used to denote a parameter that describes how microstrip exchanges power with a TEM line, just as characteristic impedance is the parameter that determines how one TEM line exchanges power with another. The purpose of this

Manuscript received September 7, 1982; revised March 15, 1983. This paper is based on work performed at COMSAT Laboratories under the shared sponsorship of the Communications Satellite Corporation and the COMPACT Engineering Division of COMSAT General Integrated Systems Corporation.

The author is with COMSAT Laboratories, Clarksburg, MD 20871.

0018-9480/83/0800-0624$01.00 ©1983 IEEE

usage is to accommodate microstrip to circuit theory and to interconnections with TEM elements, while recognizing that it is not a TEM structure itself.

This definition distinguishes the concept presented in this paper from definitions of convenience or intuition, such as those discussed by Bianco *et al.* [1] or from those based on wave impedance, as proposed previously [2]. There is wide disagreement in the microwave community about how microstrip characteristic impedance should be defined. As shown clearly by Bianco *et al.* [1], different reasonable definitions have widely different variations with frequency. The work described in this paper attempted to further resolve the question by making actual measurements of apparent characteristic impedance. Napoli and Hughes [3] made measurements intended to display microstrip characteristic impedance, but their results appear to be obscured by connector and transition reflection interactions.

Three measurement methods will be described, along with the results of measurements on microstrip lines of three nominal impedance levels. Then, mathematical models of different complexity will be discussed. First, however, some background theory will be given to explain the present confusion over the frequency variation of microstrip characteristic impedance, and illuminate the apparent impedance variations observed on measurements of microstrip lines.

II. Theoretical Background

A transmission line is completely characterized in circuit theory by characteristic impedance $Z0$, a propagation constant γ, and length l, using voltage V and current I as variables (Fig. 1). The problem to be discussed would not be avoided by employing wave formalism rather than voltage and current. If a microstrip transmission line (Fig. 2) is to be designed into circuits which also have lumped elements and TEM transmission lines, then V, I, and $Z0$ for the microstrip need to be defined to be unique and compatible with V, I, and Z of the other circuit elements.

Microwave circuit theory, which is employed in microwave frequency-domain CAD programs, such as SUPERCOMPACT™, requires that Kirchoff's voltage and current laws hold at junctions interconnecting all elements such as lumped elements, transmission lines, and other n-ports. A port can be represented by two wires carrying equal but opposite sinusoidal currents of maximum value I and having maximum sinusoidal voltage V between the wires. Then average power P entering the port is

$$P = \frac{1}{2}\,\mathrm{Re}\,VI^* \tag{1}$$

and the impedance Z presented by the port is

$$Z = V/I. \tag{2}$$

Now, P is an absolute physical quantity, but Z is relative to an arbitrary definition or reference level. That is, either V or I could be set arbitrarily and the other adjusted to give the required value of P. However, V and I of low-frequency circuit theory are related to electric and magnetic fields $\bar{E}$ and $\bar{H}$ at a port of a physical two-conductor circuit element by

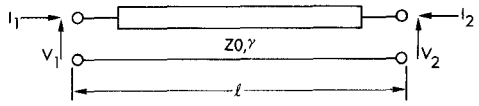

Fig. 1. Circuit theory representation of a transmission line.

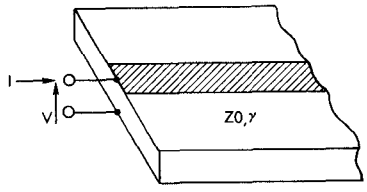

Fig. 2. Microstrip transmission line.

$$V = -\int_{C1}^{C2} \bar{E}\cdot d\bar{l} \tag{3}$$

and

$$I = \oint_C \bar{H}\cdot d\bar{l} \tag{4}$$

where the first integral is taken from one conductor ($C1$) to the other ($C2$), and the second integral is taken around one of the conductors (C). The power entering the element in terms of the fields is given by

$$P = \frac{1}{2}\,\mathrm{Re}\int_A \bar{E}\times\bar{H}^*\cdot d\bar{A} \tag{5}$$

where A is a surface through which power flows and on which the paths of integration of (3) and (4) lie. Thus, A is a terminal surface for a physical two-port. Of course, (1) and (5) must be equal if the circuit element is to be represented in circuit theory terms.

Equations (3) and (4) for voltage and current are useful because they are unique, that is, independent of the path of integration on the terminal surface. This is the case for elements, junctions, and ports which have dimensions that are small in wavelengths. These equations are special cases of Maxwell's curl equations for charge and current-free regions

$$\oint \bar{E}\cdot d\bar{l} = -\frac{\partial}{\partial t}\int_A \bar{B}\cdot d\bar{A} \tag{6}$$

$$\oint \bar{H}\cdot d\bar{l} = \int_A \bar{i}\cdot d\bar{A} + \frac{\partial}{\partial t}\int_A \bar{D}\cdot d\bar{A}. \tag{7}$$

The path of integration for (6) can be considered to go from one conductor to the other and return via a different path, thus generating the surface A over which the integral on the right is taken.

For low frequencies, the time variation of the integrands on the right of (6) and (7) is nearly zero; these equations are independent of path and equivalent to the voltage and current equations (3) and (4).

At the terminal surface of a TEM transmission line, there are no longitudinal components of the fields to contribute to the surface integrals of (6) and (7); therefore, these equations again are equivalent to the voltage and current equations. Thus, unique values of voltage and

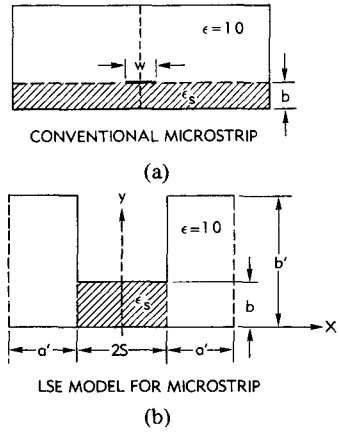

Fig. 3. (a) Conventional microstrip and (b) its LSE model.

current can be defined by (3) and (4) for the TEM line, and if it is terminated without reflection, (2) yields its characteristic impedance $Z0$.

A microstrip line, however, has longitudinal components of both electric and magnetic fields, except at zero frequency [4]; consequently, the integrals on the right of (6) and (7) cannot be neglected. Therefore, voltage and current cannot be defined independently of the path of integration by (3) and (4). Thus, (1) and (2) do not hold, and microstrip cannot be incorporated rigorously into circuit theory.

The differing variations of microstrip characteristic impedance with frequency illustrated by Bianco *et al.* [1] can be traced to the use of (3) and (4) with different paths of integration, and the fact that transverse field configurations in microstrip are not constant with frequency as they are for all homogenous transmission lines and waveguides. Nevertheless, a microstrip line is used in practical circuits with conventional lumped elements and TEM lines. Its propagation constant can be calculated by rigorous [4] or approximate [5] analytical methods or measured on the bench. Microstrip characteristic impedance at zero frequency is predictable; only its frequency variation cannot be defined uniquely. However, it appears to have a specific characteristic impedance at each frequency when measured against a transmission line of known $Z0$, as will be shown. This apparent characteristic impedance will be referred to as ZA to emphasize that it is not defined in terms of voltage and current, but in terms of its exchange of power with another circuit that can be described in terms of voltage and current.

An analytical approach to ZA is possible by sacrificing rigor and employing the longitudinal-section electric (LSE) model of microstrip [5]. This approximate model has been used to predict microstrip dispersion [5], the filling factor, and the frequency variations of different definitions of characteristic impedance [1].

Cross sections of both microstrip and the LSE model are shown in Fig. 3. The LSE model is characterized by an electric field which is entirely tangential to the air–dielectric interfaces. It is a hypothetical inhomogenous transmission line that carries a single LSE mode [6], and its zero-frequency parameters can be the same as those of the microstrip that it is to simulate. Its single-mode simplicity makes it useful for calculating the frequency behavior of microstrip parameters.

Expressions for the fields of the LSE model are given in the Appendix. It should be observed that the model has a longitudinal magnetic field but no longitudinal electric field. Therefore, (6) and hence (3) for voltage are path dependent; however, (7) and (4) defining longitudinal current are equivalent. Thus, a unique current, consistent with circuit theory, can be defined for the LSE model from its field configuration, but a unique voltage cannot. It follows that ZA for the LSE model can be defined in terms of power and current by

$$ZA = 2P/I^*I \tag{8}$$

and that voltage for the LSE model can be given by

$$V = 2P/I^*. \tag{9}$$

Equations (8) and (9) are consistent with both electromagnetic theory and circuit theory for the LSE model.

In the Appendix, an expression for ZA is derived from the fields of the LSE model in terms of commonly employed microstrip parameters. The measurements of ZA will now be discussed to investigate how well the LSE model characterizes actual microstrip transmission lines.

III. Measurement Methods and Measured Results

Three different methods were used to perform measurements on microstrip lines having nominal impedances of 32.5 Ω, 48 Ω, and 70 Ω. In each case, the microstrip line was abruptly joined to a coaxial line of known characteristic impedance, $Z1 = 50.0$ Ω. Even though the connection was abrupt, the physical discontinuity created a transition circuit between the two uniform lines as indicated in Fig. 4.

The transition circuit can be represented by a tee or pi LC network, as shown in Fig. 5. In most practical microstrip-to-coaxial-line transitions, the LC product is much less than $1/\omega^2$ at the highest frequency normally used. This constraint allows the transition circuit to be represented with reasonable accuracy by either a tee or a pi, or by an L-section of either orientation. Also, all of one element and some of the other can be made to simulate a short section of transmission line of specified impedance and can be appended to either the coaxial line or the microstrip, leaving only a single residual lumped reactance or susceptance. The lumped-element equivalences of Fig. 5 can be demonstrated comparing their $ABCD$ matrices with small terms suppressed according to $\omega^2 LC \ll 1$. The transmission-line equivalents can be demonstrated by conversion to their image-impedance lumped element representations.

The underlying philosophy of the measurement was to minimize errors and obtain maximum information about the microstrip line. To this end, the test pieces were based on a substrate 10 times thicker than the 0.025-in thick substrate widely used for microwave circuits. This increased wavelengths and reduced the effects of mechanical tolerances. It allowed the use of GR-900 connectors which have small reflections (VSWR less than $1.001 + 0.001 \times f(\text{GHz})$ per connector, used in pairs) at the reduced

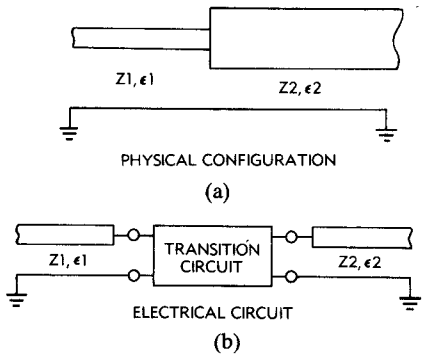

Fig. 4. Junction of dissimilar lines. (a) Physical configuration. (b) Electrical circuit.

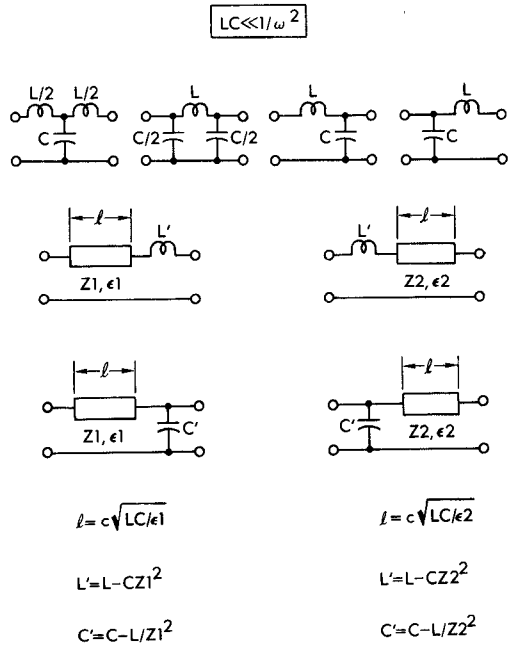

Fig. 5. Equivalent transition circuits for $LC \ll 1/\omega^2$.

frequency range so that their effect on the measurements could be neglected.

The microstrip lines used for the measurements were defined by photolithography using electroless copper-plated alumina substrates $2.0 \times 10.0 \times 0.25$-in size, and having a dielectric constant of 9.74 measured at low frequency. The final metallization thickness was about 1.3 mils. In most cases, the conductors were gold-flashed to ensure good contacts. The substrate enclosure was an aluminum bed with removable sides that held the substrate against the bed by means of small ridges. These sides extended about 1.5 in above the substrate. A metal top was available for the substrate enclosure, but was seldom used because it had negligible effect below about 3 GHz, and above that frequency accentuated the effects of higher mode resonances. The ends of the enclosure were tapped to accept either a GR-900 connector or a flat copper plug. With a copper plug in place, the microstrip was effectively terminated at that end by a flat plate short with no discontinuity effect.

With copper plugs at both ends, the microstrip could be

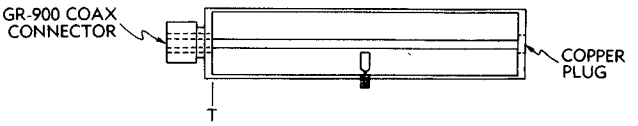

Fig. 6. Microstrip test piece.

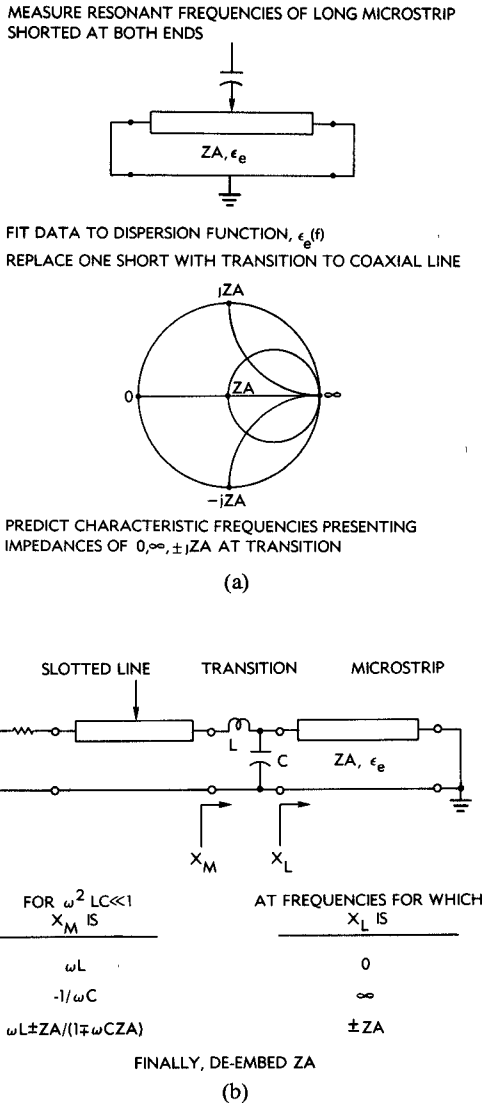

Fig. 7. (a) Slotted line method (dispersion measurement). (b) Slotted line method (transition and impedance measurement).

resonated with a temporary stub attached to an OSM connector in the side of the enclosure midway along the line, as shown in Fig. 6. By observing reflection coefficient dips, resonant frequencies were measured for two gap widths, and the results extrapolated for infinite gap width. Alternatively, at each resonance, the gap width was gradually increased and the frequency observed at which the resonant dip approached the swept frequency baseline. The microstrip line widths were 0.10, 0.25, and 0.50 in.

Three measurement methods were tested; they are denoted as the slotted line, the real-axis intercept, and the group-delay methods. The slotted line method is outlined in Fig. 7. First, the copper plugs are used to terminate the microstrip at both ends with flat plate shorts. Resonant frequencies are measured and, if necessary, corrected for

probe capacitance. These frequencies are investigated graphically versus the order of the resonance for smoothness and used to compute the frequency dependent effective dielectric constant ϵ_e

$$\epsilon_e = \left(\frac{nc}{2fl}\right)^2 \tag{10}$$

where n is the number of half-wavelengths along the line, c is the speed of light in vacuum, f is the resonant frequency, and l is the length of the line.

The discrete values of ϵ_e are fitted to any appropriate mathematical function to allow prediction of ϵ_e with frequency. Then, when one copper plug is replaced by a GR-900 connector, frequencies can be predicted for which the shorted line presents (lossless assumption) shorts, opens, or $\pm jZA$ at the junction with the connector, as indicated on the Smith chart of Fig. 7(a). Reactance at each of these frequencies is measured with a GR-900 slotted line, using a shorted coaxial reference to define the terminal plane at the connector end of the microstrip.

A slotted line is used because it eliminates equipment calibration; only distance and frequency are measured. The stability of a synthesizer makes frequency errors negligible. Uncertainty in distance is about ± 0.1 mm, or less than 0.1 percent, in wavelengths at 2 GHz. The author believes that most of the scatter in this type of measurement arises not from the measuring equipment or technique, but from the test piece itself. Possible sources of error are inhomogeneity of the substrate, imperfect uniformity of the line width, and extraneous resonance effects resulting from contact problems, particularly with the ground plane.

As indicated in Fig. 7(b), the reactance measurements yield ωL, $-1/\omega C$, and $\omega L \pm ZA/(1 \mp \omega CZA)$ allowing ZA to be determined. The values of L and C found were small [7], justifying the use of a two-element transition circuit in accordance with Fig. 5. Although not illustrated in this paper, both L and C of the transition appeared to increase with frequency [7]. This is believed to be caused by the change with frequency of the field configuration of microstrip as the power becomes more concentrated in the dielectric-filled part of the line.

The results of measurements on a 0.25-in-wide line are shown in Fig. 8. Point-by-point values of L and C were used to de-embed ZA for one curve and best-fit constant values of L and C for the other curve.

If there is a consistent error in the value used for L or C, values found for ZA at consecutive measured frequencies will alternate above and below the correct value. When this saw-toothed effect is found in the reduced data, the best value for ZA lies halfway between alternating consecutive points.

Fig. 8 illustrates a characteristic that will be found for ZA measurements of all lines by all methods. First, there is a gradual decrease in ZA with frequency followed by an increase to beyond the zero-frequency value of ZA as frequency continues to rise.

The real-axis intercept method of measurement is illustrated in Fig. 9. A long, uniform, symmetrical microstrip

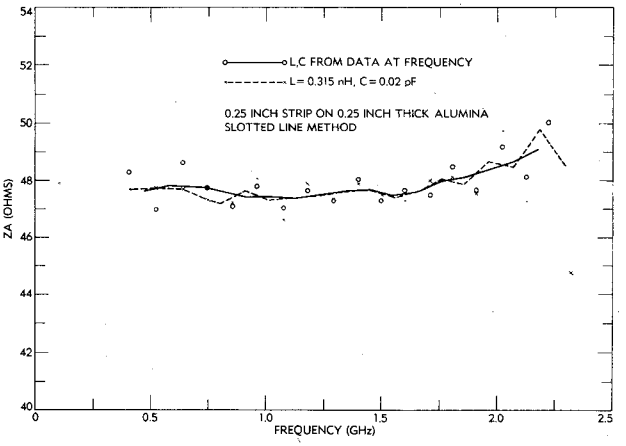

Fig. 8. Measured ZA of 0.250-in line by slotted line method.

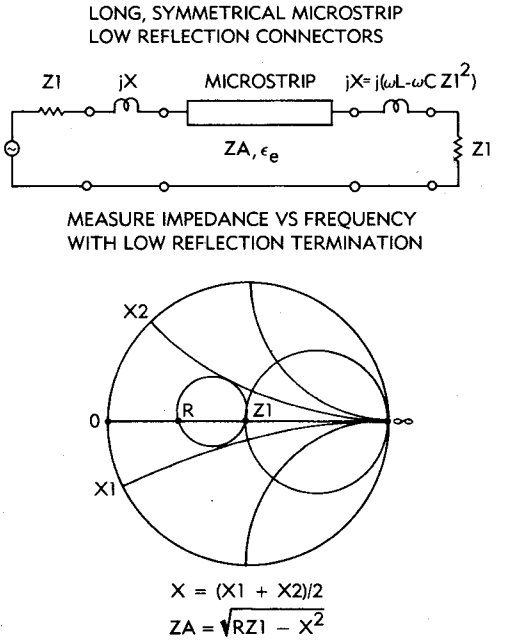

Fig. 9. Real-axis intercept method.

is placed in a measuring system having very low internal reflections, including connectors and a matched load. As pointed out in the discussion on transitions (Fig. 5), the transition circuit can be incorporated into the transmission line external to the microstrip, except for a single residual reactance or susceptance. This measurement arrangement can be represented by the circuit of Fig. 9.

Conventional circuit analysis indicates that as frequency is swept, the input impedance makes nearly circular spirals on the Smith chart. $X1$ and $X2$ are the extreme values of reactance whose algebraic average X is the residual reactance of the transition; that is, $X = (X1 + X2)/2$. On each rotation, the spiral passes through the center of the Smith chart and crosses the real impedance axis again at some value R. Solution of the expression for input impedance of the circuit of Fig. 9 for zero imaginary part yields the value R. Rearrangement of the result gives ZA as

$$ZA = \sqrt{R \cdot Z1 - X^2}. \tag{11}$$

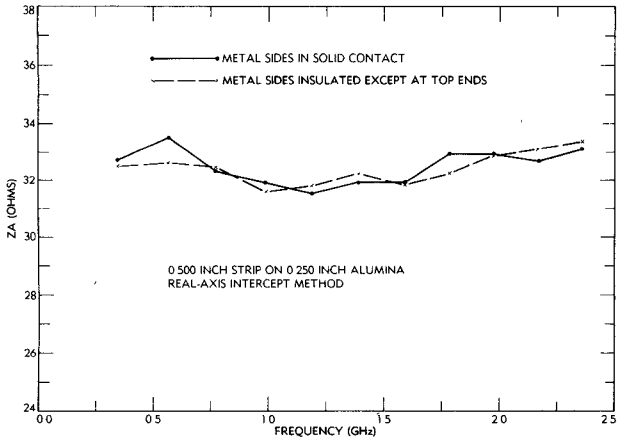

Fig. 10. Measured ZA of 0.500-in line by real-axis intercept method.

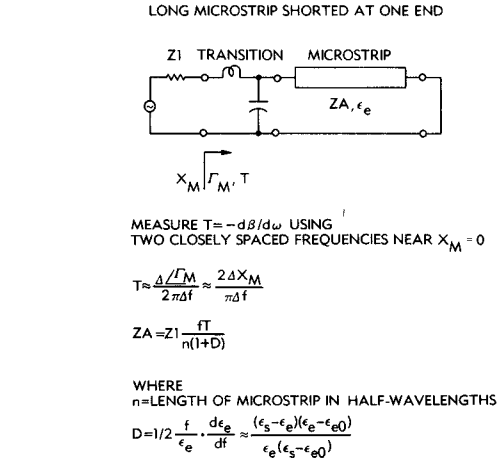

Fig. 11. Group-delay method.

Rigorously, X^2 should be referred to the frequency at which R was measured; however, in practice, it was found to be small enough to be neglected altogether. If R is near $Z1$, the impedance locus is nearly parallel to the real axis, and a small internal reflection in the measuring system can cause a significant error in the real-axis crossing. Thus, poor accuracy would be expected for $ZA \approx Z1$.

Fig. 10 shows the results of real-axis intercept measurements on a strip 0.5-in wide. The decline, then rise, of impedance with frequency is similar to that observed for the 0.25-in-wide line using the slotted line method. For one set of measurements, the contact of the enclosure sides was broken, except at the top ends, to perturb any surface wave or higher mode currents. No significant effect was observed up to 3 GHz.

The group-delay method of measuring ZA is important because it is almost independent of the transition, and it is relatively simple to perform. As is illustrated in Fig. 11, it requires a relatively long microstrip terminated with a flat plate short. The reflection delay [8] T is measured about frequencies for which the shorted microstrip presents zero reactance X at the transition.

$$T = -\frac{d\beta}{d\omega} = -\frac{1}{2\pi}\cdot\frac{d\angle\Gamma}{df} \approx \frac{2}{\pi Z1}\cdot\frac{dX}{df}. \tag{12}$$

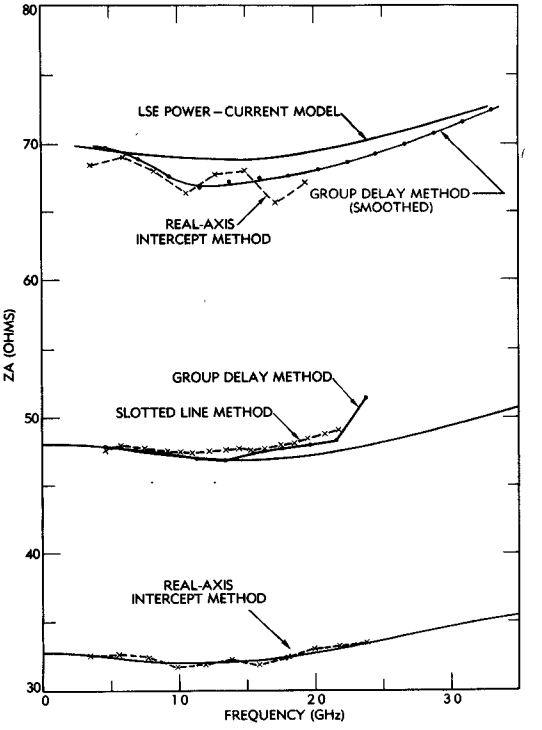

Fig. 12. Measured ZA of three line widths by three methods.

In (12), β represents the total phase shift of the reflected wave with respect to the incident wave (i.e., the angle of the reflection coefficient Γ), measured at the input port.

ZA is given by

$$ZA = Z1\frac{fT}{n(1+D)} \tag{13}$$

where n, an integer, is the length of the microstrip in half-wavelengths at f and

$$D = \frac{1}{2}\cdot\frac{f}{\epsilon_e}\cdot\frac{d\epsilon_e}{d_f} \approx \frac{(\epsilon_s-\epsilon_e)(\epsilon_e-\epsilon_e(0))}{\epsilon_e(\epsilon_s-\epsilon_e(0))} \tag{14}$$

where ϵ_s is the substrate relative dielectric constant, and $\epsilon_e(0)$ is the effective dielectric constant at zero frequency. The final term in (14) was derived from the approximate expression for ϵ_e developed in [5].

Equation (13) was derived by taking the derivative with respect to frequency of the input reflection coefficient or reactance of the shorted microstrip, including the rate of change of the effective dielectric constant, for those frequencies at which the input reactance is zero.

One measurement technique used by the author was to find the small frequency difference needed for a specified reflection phase difference observed on a network analyzer, and to approximate the terms of (12) with differentials.

Fig. 12 shows ZA measurements for lines 0.1-, 0.25-, and 0.5-in wide on the 0.250-in-thick alumina substrate. ZA for all lines has the decline and rise characteristic observed previously. The agreement of the different measurement methods is considered quite satisfactory.

In summary, it can be observed that the slotted line method gives the most information—dispersion, transition elements, and ZA—but is the most difficult to perform

and from which to de-embed ZA. The real-axis intercept method is the easiest to make and from which to find ZA, but requires excellent connectors and load. The group-delay method, because it tends to "look through" the transition and connector, is probably the best method for use at actual microwave frequencies, and most likely could be automated for faster measurements, if necessary. Also, the delay data can be smoothed on a piecewise-linear basis as was done for the 70-Ω line shown in Fig. 12.

Measurements of ZA from about 3 to 5 GHz showed excessive variations caused by coupling to undesired modes. The LSM_{11}-mode cutoff frequency was found by both calculation and measurement to occur near 3 GHz.

IV. Models of ZA

The first and simplest microstrip characteristic impedance model is the constant impedance model which approximates ZA by its zero-frequency value

$$ZA(f) = ZA(0). \tag{15}$$

This is a practical approximation because actual ZA decreases only by about 2 percent and rises to the zero-frequency value again at about the maximum frequency at which the substrate would be used. For example, an alumina substrate 0.025-in thick would be used up to a maximum of 18 GHz, typically.

The next simplest model is the wave impedance model [2], so-called because it describes the characteristic impedance variation with frequency of any mode on a homogeneous transmission line. For microstrip, this would require ZA to be proportional to the reciprocal of the square root of the effective dielectric constant

$$ZA(f) = ZA(0)\sqrt{\epsilon_e(0)/\epsilon_e(f)}\,. \tag{16}$$

The wave impedance model for ZA follows the measurements in the lower frequency range more accurately than the constant impedance model, but continues to decline even when measured ZA reverses its slope.

The LSE model predicted that the power-current impedance definition could be expected to describe microstrip ZA approximately; however, "goodness of fit" could be determined only by measurement. As shown in Fig. 12, the power-current model has zero slope at zero frequency, declines to a broad minimum of about the same value at about the same frequency as the measurements, and increases thereafter at about the same slope.

A derivation of an algebraic expression for the LSE power-current model of ZA is given in the Appendix. The result, while easily programmed, is too complicated for evaluation by a hand calculator. A simpler expression, termed the group-delay model is found by replacing f/n in (13) by its equivalent determined from (10), and then forming the ratio $ZA(f)/ZA(0)$

$$\frac{ZA(f)}{ZA(0)} = \frac{T(f)}{T(0)} \cdot \frac{\sqrt{\epsilon_e(0)/\epsilon_e(f)}}{1+D(f)}. \tag{17}$$

Making the heuristic assumption that

$$\frac{T(f)}{T(0)} \simeq \frac{\epsilon_e(f)}{\epsilon_e(0)} \tag{18}$$

results in

$$ZA = ZA(0)\frac{\sqrt{\epsilon_e/\epsilon_e(0)}}{1+D}. \tag{19}$$

This approximate formula is a close fit to the LSE power-current model to well beyond the frequency at which ZA rises through $ZA(0)$.

Approaching infinite frequency, the group-delay model becomes

$$ZA(\infty) = ZA(0)\sqrt{\epsilon_s/\epsilon_e(0)} \tag{20}$$

while the LSE power-current model becomes

$$ZA(\infty) = ZA(0)\cdot\frac{\pi^2}{8}\cdot\sqrt{\frac{\epsilon_e(0)}{\epsilon_s}}\cdot\frac{\epsilon_s-1}{\epsilon_e(0)-1}. \tag{21}$$

These differ by about 30 percent for a 50-Ω line on alumina. Derivation of (21) is discussed in the Appendix.

V. Discussion

Repeatability of impedance measurements was within about 0.5 percent. Scatter varied from about 0.5 percent to 2 or 3 percent, and occasionally more. It was greater for the 70-Ω test pieces than for the others. Above 3 GHz, higher mode coupling was clearly a major source of error. Some ideas about measurement error were given in the section on measurements. In general, there appeared to be a number of causes of scatter, but they were not tracked down.

Differences between the actual measurements and the LSE power-current (or group-delay) model arise from three possible sources: the actual microstrip is not ideal (inhomogeneities of substrate and line width, and contact problems); measurements are not ideal (effect of small reflections and instrument calibrations); or the model only approximates microstrip (other coupled modes not included). No attempt has been made to separate the errors from these sources at this time (below 3 GHz).

The surprisingly large frequency variation of the measured impedance of the 70-Ω line and its deviation from the model are unexplained and indicate the need for corroborative investigation. However, of the ZA models described, the LSE power-current model is the most faithful over the widest frequency range to the characteristics measured on actual microstrip and has sufficient accuracy for microstrip circuit design.[1]

[1] One of the reviewers of this paper has proposed that other power-current models of microstrip might give better results than the LSE model, and suggests specifically computations based on the actual microstrip field [12], and the planar waveguide model with frequency dependent effective width [13]. The author believes that such a comparison of models (with relation to experimental results) would be a useful investigation, but is beyond the scope of this paper.

This conclusion is supported by the work of Jansen and Koster [9], who found that a hybrid-mode numerical analysis of junctions between microstrips of different widths agreed best with circuit representations when a power-current definition of ZA was assumed. Their work also tends to confirm that ZA is the same for a microstrip-to-microstrip junction as for a coaxial line-to-microstrip junction. Thus, Bianco's suggestion of a frequency-sensitive ideal transformer at the transition [10], while mathematically possible, need not be invoked.

The power-current LSE model probably holds only for thin strips which, with their ground planes, are in intimate contact with their substrates. It would not be likely to hold for suspended substrate lines or thick center conductors [11], because the LSE assumption (electric field tangential at the interface) would not hold as well, and so neither voltage nor current could be defined uniquely.

Appendix
Power-Current Impedance Analysis

The power-current definition of the characteristic impedance ZA of the LSE model for microstrip is derived below.

Following Collin [6], a Hertzian vector $\bar{\pi}$ in the x-direction with a wave function ψ is used to determine the fields of the fundamental LSE (or TE, in this case) mode in the structure of Fig. 3, assuming propagation in the z-direction. Let

$$\bar{\pi} = \hat{x}_0 \psi_i e^{-\gamma z} \tag{A1-a}$$

$$\psi_i = \frac{B_i}{\omega^2} \cosh \gamma_i x_i \tag{A1-b}$$

in which

$\hat{x}_0$	unit vector along the x-axis;	
$\gamma = j(\omega/c)\sqrt{\epsilon_e}$	propagation constant;	(A1-c)
ω	radian frequency;	
c	speed of light in vacuum;	
ϵ_e	frequency dependent effective dielectric constant;	
i	index denoting dielectric (1) or air (2) regions;	
ϵ_i	dielectric constant of the region i, $\epsilon_1 = \epsilon_s$ and $\epsilon_2 = 1$;	(A1-d)
$\gamma_i^2 = (\omega/c)^2 (\epsilon_e - \epsilon_i)$	transverse (x-directed) propagation constant in the region i; and a constant.	(A1-e)

Also

$$x_1 = x \qquad \text{for } 0 \leqslant x \leqslant s \tag{A1-f}$$

and

$$x_2 = s + a' - x \text{ for } s \leqslant x \leqslant s + a'. \tag{A1-g}$$

The term ω^2 introduced into the denominator of (A1-b) prevents the fields from disappearing at zero frequency.

It can be shown [6] that

$$\bar{E} = -j\omega\mu \nabla \times \bar{\pi} \tag{A2-a}$$

and

$$\bar{H} = \nabla \nabla \cdot \bar{\pi} + k_i^2 \bar{\pi} \tag{A2-b}$$

where μ is the permeability of free space, that

$$k_i^2 = \left(\frac{\omega}{c}\right)^2 \epsilon_i \tag{A2-c}$$

and that the propagation constants are related by

$$\gamma^2 + \gamma_i^2 + k_i^2 = 0. \tag{A2-d}$$

An approximate solution for γ was found in [5]. It follows that with z-variation suppressed, the fields are

$$E_x = E_z = 0 \tag{A2-e}$$

$$E_{y_i} = j\frac{\mu\gamma B_i}{\omega} \cosh \gamma_i x_i \tag{A2-f}$$

$$H_{x_i} = -\frac{B_i \gamma^2}{\omega^2} \cosh \gamma_i x_i \tag{A2-g}$$

$$H_y = 0 \tag{A2-h}$$

$$H_{z_i} = (-1)^i \frac{\gamma \gamma_i B_i}{\omega^2} \sinh \gamma_i x_i. \tag{A2-i}$$

Power in the z-direction, P of (5), can be written in terms of the fields as

$$P = -\frac{1}{2} \operatorname{Re} \int E_y H_x^* \, dx \, dy. \tag{A3}$$

The wave impedance Z_w is

$$Z_w = -\frac{E_y}{H_x} = \frac{j\omega\mu}{\gamma} \tag{A4}$$

which is independent of position or region on a transverse surface [2].

Now, substituting (A4) into (A3), and integrating over dielectric and air regions separately gives

$$P = \frac{j\omega\mu}{\gamma}\left[\int_0^b \int_0^s |H_{x_1}|^2 \, dx \, dy + \int_0^{b'} \int_s^{s+a'} |H_{x_2}|^2 \, dx \, dy\right]. \tag{A5}$$

Similarly, an expression for longitudinal current I on the conductors of both regions is

$$I = 2\int_0^s H_{x_1} dx + 2\int_s^{s+a'} H_{x_2} dx. \tag{A6}$$

Now, if the z-directed magnetic fields are matched at the air–dielectric interface, the electric potential will also be matched if γ is maintained in agreement with the transverse resonance condition in [5, (8)]. Matching the H_{zi} gives

$$B_1 \gamma_1 \sinh \gamma_1 s = -B_2 \gamma_2 \sinh \gamma_2 a'. \tag{A7}$$

Employing (A1-d) and (A1-e) and rearranging gives

$$\frac{B_2}{B_1} = \sqrt{\frac{\epsilon_s - \epsilon_e}{\epsilon_e - 1}} \cdot \frac{\sin(\omega/c)\sqrt{\epsilon_s - \epsilon_e}\, s}{\sinh(\omega/c)\sqrt{\epsilon_e - 1}\, a'}. \tag{A8}$$

The power-current definition of apparent characteristic impedance ZA was given in (8) of the text. Equations (A5)

and (A6) are substituted into (8), using (A2-g) and (A8), and the resulting expression is simplified by employing equalities of the following form:

$$\operatorname{sinc}|\gamma_1|s = \frac{\sin(\omega/c)\sqrt{\epsilon_s-\epsilon_e}\,s}{(\omega/c)\sqrt{\epsilon_s-\epsilon_e}\,s} \tag{A9-a}$$

$$\operatorname{sinch}\gamma_2 a' = \frac{\sinh(\omega/c)\sqrt{\epsilon_e-1}\,a'}{(\omega/c)\sqrt{\epsilon_e-1}\,a'}. \tag{A9-b}$$

This leads to the final relationship for ZA, the power-current characteristic impedance of the LSE model

$$ZA = \frac{\eta_0 b/s}{4\sqrt{\epsilon_e}} \left\{ \frac{(1+\operatorname{sinc}2|\gamma_1|s) + \dfrac{a'b'}{bs}\dfrac{\epsilon_s-\epsilon_e}{\epsilon_e-1} \cdot \left(\dfrac{\sin|\gamma_1|s}{\sinh\gamma_2 a'}\right)^2 (1+\operatorname{sinch}2\gamma_2 a')}{\left[\operatorname{sinc}|\gamma_1|s + \dfrac{a'}{s}\sqrt{\dfrac{\epsilon_s-\epsilon_e}{\epsilon_e-1}} \cdot \left(\dfrac{\sin|\gamma_1|s}{\sinh\gamma_2 a'}\right)\operatorname{sinch}\gamma_2 a'\right]^2} \right\} \tag{A10}$$

where η_0 is the impedance of free space. The relations [5, (4a) and (4b)] are, in the notation of this paper

$$\frac{a'}{b'} = \frac{\eta_0}{2ZA(0)\sqrt{\epsilon_e(0)}} \cdot \frac{\epsilon_s-\epsilon_e(0)}{\epsilon_s-1} \tag{A11-a}$$

$$\frac{s}{b} = \frac{\eta_0}{2ZA(0)\sqrt{\epsilon_e(0)}} \cdot \frac{\epsilon_e(0)-1}{\epsilon_s-1}. \tag{A11-b}$$

Use of (A11-a) and (A11-b) will leave the factor b'/b to be evaluated. This quantity must be found experimentally for microstrip, as observed in [5].

When (A11-a) and (A11-b) are substituted into (A10) and frequency allowed to approach zero, all sinc and sinch tend to unity, and $\sin|\gamma_1|s/\sinh\gamma_2 a'$ becomes

$$(s/a')\sqrt{(\epsilon_s-\epsilon_e(0))/(\epsilon_e(0)-1)}\,.$$

The predicted zero-frequency impedance is

$$ZA(0) = \frac{\eta_0 b/s}{2\sqrt{\epsilon_e(0)}} \cdot \frac{\epsilon_e(0)-1}{\epsilon_s-1}. \tag{A12}$$

This can be seen to be equivalent to a rearrangement of (A11-b), which was derived in [5] by forcing agreement between microstrip and LSE parameters at zero frequency. Thus, $ZA(0)$ is the same as static determinations of microstrip characteristic impedance.

The apparent power-current characteristic impedance at infinite frequency $ZA(\infty)$ is found by observing that the second terms of both denominator and numerator of (A10) go to zero, and that γ_1 is indeterminate. The indeterminacy is resolved by appeal to the transverse resonance relation [5, (8)], which requires that $|\gamma_1|s \to \pi/2$ as $\omega \to \infty$. The result is given in (21).

Equations (A10), (A12), and (21) show that ZA is indeterminate for $\epsilon_s = \epsilon_e(0) = 1$. This occurs because dimensions are related to impedance by means of ratios of differences of dielectric constants for the LSE model. Resolution of the indeterminacies would require knowledge of the functional relation between $\epsilon_e(0)$ and ϵ_s as ϵ_s approaches unity.

Acknowledgment

The author is pleased to express his thanks to A. Berman of COMSAT Laboratories, and to S. March of COMPACT Engineering, CGIS, for their helpful technical discussions and continuing support during the course of the work.

References

[1] B. Bianco *et al.*, "Some considerations about the frequency dependence of the characteristic impedance of uniform microstrips," *IEEE Trans. Microwave Theory Tech.*, vol. MTT-26, pp. 182–185, Mar. 1978.

[2] W. J. Getsinger, "Microstrip characteristic impedance," *IEEE Trans. Microwave Theory Tech.*, vol. MTT-27, p. 293, Apr. 1979.

[3] L. Napoli and J. Hughes, "High frequency behavior of microstrip transmission lines," *RCA Rev.*, vol. 30, pp. 268–276, June 1969.

[4] M. K. Krage and G. I. Haddad, "Frequency dependent characteristics of microstrip transmission lines," *IEEE Trans. Microwave Theory Tech.*, vol. MTT-20, pp. 678–688, Oct. 1972.

[5] W. J. Getsinger, "Microstrip dispersion model," *IEEE Trans. Microwave Theory Tech.*, vol. MTT-21, pp. 34–39, Jan. 1973.

[6] R. E. Collin, *Field Theory of Guided Waves*. New York: McGraw-Hill, 1960, pp. 225–228.

[7] W. J. Getsinger, "Measurement of the characteristic impedance of microstrip over a wide frequency range," in *IEEE MTT-S Int. Microwave Symp. Dig.*, June 1982, pp. 342–344.

[8] S. J. Mason and H. J. Zimmermann, *Electronic Circuits, Signals and Systems*. New York: Wiley, 1965, pp. 366–369.

[9] R. H. Jansen and N. H. Koster, "New aspects concerning the definition of microstrip characteristic impedance as a function of frequency," in *IEEE MTT-S Int. Microwave Symp. Dig.*, pp. 305–307, June 1982.

[10] B. Bianco *et al.*, "Launcher and microstrip characterization," *IEEE Trans. Instrum. Meas.*, vol. IM-5, pp. 320–323, Dec. 1976.

[11] F. Arndt and G. Paul, "The reflection definition of the characteristic impedance of microstrips," *IEEE Trans. Microwave Theory Tech.*, vol. MTT-27, pp. 724–731, Aug. 1979.

[12] T. Itoh and R. Mittra, "A technique for computing dispersion characteristics of shielded microstrip lines," *IEEE Trans. Microwave Theory Tech.*, vol. MTT-22, pp. 896–898, Oct. 1974.

[13] H. Pues and A. Van de Capelle, "Approximate formulas for frequency dependence of microstrip parameters," *Electron. Lett.*, vol. 16, no. 23, pp. 870–872, Nov. 6, 1980.

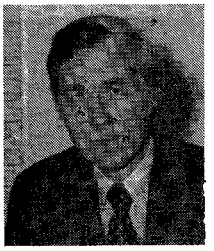

William J. Getsinger (S'48–A'50–M'55–SM'69–F'81) was born in Waterbury, CT, in 1924. He received the B.S. degree from the University of Connecticut in 1949, the M.S. degree and the degree of Engineer in 1959 and 1961 from Stanford University, all in electrical engineering.

Since 1957 he has worked in microwave circuit research and development at Stanford Research Institute, M.I.T. Lincoln Laboratory, and at COMSAT Laboratories. He joined COMSAT in 1969 as a Department Manager. In 1981 he was named a Senior Scientist at COMSAT.